Energy Level Alignment at Metal−Octaethylporphyrin Interfaces

A. Alkauskas,*,† L. Ramoino,†,‡ S. Schintke,† M. von Arx,† A. Baratoff,† H.-J. Güntherodt,† and T. A. Jung†,§

NCCR Nanoscale Science, Institute of Physics, University of Basel, Klingelbergstrasse 82, CH-4056 Basel, Switzerland, and Laboratory for Micro- and Nanotechnology, Paul Scherrer Institute, CH-5232 Villigen, Switzerland

Received: August 4, 2005; In Final Form: October 11, 2005

We studied the electronic structure of copper−octaethylporphyrin (CuEOP) adsorbed on three metal surfaces—Ag(001), Ag(111), and Cu(111)—by means of ultraviolet photoelectron spectroscopy (UPS). The adsorption-induced work function shifts saturate roughly beyond two monolayers. The saturation values are substrate dependent, negative, and range from −1.30 to −0.85 eV. This shift is larger than that for tetraphenylporphyrins. The two highest occupied molecular orbitals (HOMO and HOMO-1) of the organic are clearly resolved in the UPS spectra. The origin of the negative work function shift is discussed.

1. Introduction

Understanding the electronic structure of metal−organic interfaces is of high current interest, being motivated by the appearance of hybrid organic−inorganic electronic and optical devices,[1,2] such as organic light-emitting diodes (OLEDs) and organic thin film transistors.[3] Detailed control of the interfacial electronic structure is necessary to improve the efficiency of charge carrier injection from the metal to the organic semiconductor. Studies of metal−molecule contact properties and interfacial electrostatics gained renewed attention in recent years, particularly in the context of molecular electronics, where transport ultimately occurs through a single molecule.[4] Charge transfer, energy barriers, and energy level alignment at interfaces are of great importance in those contexts.[5,6,10]

Permanent or adsorption-induced dipoles with a perpendicular component at the interface shift the vacuum level (VL) or, equivalently, the work function (WF) of the composite sample. Therefore the position of the molecular levels with respect to the Fermi level E_F of the metallic substrate deviates from the naive picture of vacuum level alignment. Detailed reviews of general principles and experimental examples of representative systems are given by Ishii et al.,[7,8] as well as by Knupfer and Peisert.[9] A schematic energy level diagram is shown in Figure 1. The relevant parameters which can be determined by ultraviolet photoelectron spectroscopy (UPS) are Φ_m, the metal work function, IP, the ionization potential of the molecular thin film, ϵ_F^v, the energy of the highest occupied molecular orbital (HOMO) with respect to the substrate Fermi level E_F, and Δ, the VL shift. The four quantities are related by

$$\epsilon_F^v = \Phi_m + \Delta - \mathrm{IP} \qquad (1)$$

ϵ_F^v is negative in such a definition. This picture neglects a possible band bending in the organic layer, and does not include interfacial states, i.e., the hybrid states formed at the interface in the presence of chemical interactions which occur with more reactive metals, like Ti, In, and Sn.[11]

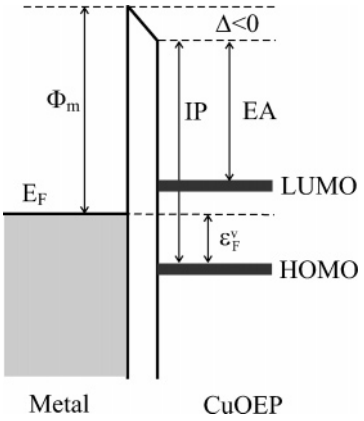

Figure 1. Schematic diagram of electronic levels at a metal−organic interface. Φ_m is the work function of the bare metal surface, Δ is the vacuum level (VL) shift, IP and EA are the ionization potential and the electron affinity of the molecular layer, ϵ_F^v is the position of the highest occupied molecular orbital with respect to the Fermi level, and E_F is the Fermi level of the metal.

Typically (as long as the ionization potential of the molecule is not particularly large and the work function of the metal is not too small) one observes a downward shift of the VL[12] ($\Delta < 0$). Several notable exceptions where the work function increases ($\Delta > 0$) are, e.g., *N*,*N*′-diphenyl-1,4,5,8-naphthalene-tetracarbocylimide (DP-NTCI) on Al,[13] tetracyanoquinodimethane (TCNQ) on Au and Al,[7] or 3,4,7,8-perylene-tetracarboxylic-dyanhidride (PTCDA) on Mg, In, and Sn.[12] These molecules have large electron affinities (EAs), as well as ionization potentials (IPs),[3] and are known to be electron acceptors.

Changing the chemical composition of the side groups of the organic molecule can influence the gas-phase IP and/or EA. This also modifies electron accepting and donating properties of adsorbed overlayers and, as a result, charge transfer at the interface, hence Δ. For example, Peisert et al.[14,15] observed that peripheral fluorination of copper phthalocyanine leads to an increase of the IP of molecular films by up to 1.1 eV, which

* Address correspondence to this author. E-mail: audrius.alkauskas@unibas.ch.
† University of Basel.
‡ E-mail: luca.ramoino@unibas.ch.
§ Paul Scherrer Institute.

10.1021/jp054325j CCC: $30.25
Published on Web 11/23/2005

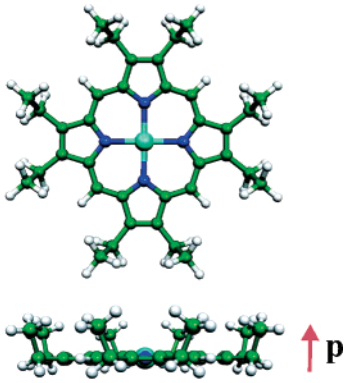

Figure 2. The structure of the CuOEP molecule: top view (above) and side view (below). In this particular configuration with all ethyl "legs" pointing up, CuOEP possesses a small calculated dipole moment $p \approx 0.45$ D.

can even result in a reversal of Δ. Campbell et al.[16,17] have demonstrated that monolayers of organic molecules with a permanent dipole sandwiched between the metallic substrate and the active organic material lead to a VL shift. The resulting energy barrier at the interface can either improve or deteriorate charge carrier injection, thus opening a way to engineer interfacial electronic properties.[18,19]

In this work, we have studied copper−octaethylporphyrin (CuOEP) adsorbed on three metal surfaces, Ag(111), Ag(001), and Cu(111), by means of UPS. CuOEP (Figure 2) consists of one porphine ring and eight ethyl groups attached to all β positions. Several recent works concentrated on the properties of octaethylporphyrins on similar substrates. Scudiero et al.[20] obtained a high quality monolayer of NiOEP on Au(111) and characterized it by scanning tunneling microscopy (STM), X-ray photoelectron spectroscopy (XPS), and UPS. The VL shift, however, was not discussed in that work. Impressive bimolecular self-assembled monolayers of NiOEP intermixed with perfluorinated cobalt phthalocyanine ($CoF_{16}Pc$)[21] and CuOEP intermixed with cobalt phthalocyanine (CoPc)[22] were demonstrated by different groups. Very recently, epitaxial layers of CuOEP on ultrathin NaCl films predeposited on Ag(001), Ag(111), and Cu(111) were obtained and studied in our laboratory.[23]

The interfacial electronic structure of other porphyrins, i.e., tetraphenylporphyrin (H_2TPP), zinc-tetraphenylporphyrin (ZnTPP), and tetra(4-pyridil)porphyrin (H_2(4-Py)TPP) were studied by Seki and co-workers.[13,24] An almost substrate-independent VL shift of about −0.6 eV was found for ZnTPP, whereas the VL shifts ranged from −0.3 to −1.0 eV for H_2TPP and from −0.1 to −0.6 eV for (H_2(4-Py)TPP), depending on the substrate. As mentioned by Scudiero et al.,[20] small β-alkyl substituents allow for a shorter distance between the metal surface and the porphine ring, thus for CuOEP on metallic substrates one expects a stronger molecule−substrate interaction.

2. Experimental Section

All experiments have been performed at room temperature in a multichamber UHV system (base pressure 1×10^{-10} mbar) allowing in situ sample preparation and characterization. CuOEP was deposited on three different single-crystal substrates: Ag(001), Ag(111), and Cu(111) (Mateck GmbH, Jülich, Germany). Atomically clean and flat surfaces have been prepared by cycles of Ar^+ sputtering and annealing, as crosschecked by STM and XPS. CuOEP deposition is achieved by sublimation from a tantalum crucible with deposition rates of 0.5−1.0 ML/min. During deposition and analysis the sample is kept at room temperature. Samples of different CuOEP coverage (up to a few layers) with special focus on the submonolayer range have been systematically investigated by UPS and XPS at normal emission, as well as by STM and low energy electron diffraction (LEED).

The layer thickness is deduced from the deposition rate monitored by a quartz microbalance, which has been calibrated from STM and XPS measurements at submonolayer coverage. On all three substrates, the first CuOEP layer shows epitaxial growth and the superstructures have been determined from LEED and STM measurements.[25] For higher thicknesses, the indicated "nominal coverage" refers to the quartz mircrobalance calibration assuming the same sticking probability also for further layers. We note, however, that in the multilayer regime this approximation is likely to overestimate the real CuOEP coverage. In particular, XPS indicates that this overestimation is larger for Ag(111) and Ag(001) than for Cu(111). Consistently, LEED measurements show that CuOEP multilayers (nominal coverage of 15 ML) on Ag substrates have the same crystalline structure as the first monolayer, while they show diffuse scattering without recognizable features on Cu(111). Thus, LEED and XPS measurements indicate that for CuOEP multilayers the real coverage is difficult to estimate. However, as shown later, the work function shifts, which we are interested in, do not significantly depend on the CuOEP coverage beyond the second monolayer.

UPS measurements have been performed with a VG ESCALAB MKII instrument, using a helium lamp operating on the HeI_α line (21.2 eV) as the UV source and a hemispherical 150° analyzer with three channeltron electron counters as the detector. To measure the work function of the CuOEP/metal systems a negative voltage (−10 V) was applied to the sample. This allows us to measure the whole width of the UPS spectrum including the low kinetic energy cutoff of the emitted secondary photoelectrons. The work function is then determined according to the relationship

$$h\nu = W + \Phi \tag{2}$$

where W is the spectral width (distance from the Fermi edge to the secondary-electron cutoff), and Φ is the sample work function.[7] The same experimental setup was used in earlier studies for the measurement of the work function shifts.[26]

3. Computations

To help to interpret measured spectra, we performed density functional calculations of the free CuOEP molecule using the Gaussian program package.[27] The hybrid B3LYP functional was employed with a 6-311G basis set for the light atoms and the Lanl2DZ effective core potential and basis set for the copper atom. Due to the flexibility of the ethyl side groups, several conformers exist. The differences in ground state energies of different conformers are very small (a few meV), however. Rotations of the alkyl "legs" practically do not influence the frontier orbitals (as is expected of their π-character) and only affect states located more than 3 eV below the HOMO. As concluded from STM measurements,[25] each CuOEP adopts a conformation with all eight "legs" pointing up in the first overlayer (Figure 2). In that conformation the molecule possesses a C_{4v} symmetry, without inversion. As for other porphyrins,[29,30] the HOMO is composed of two near-degenerate orbitals of a_1 and a_2 symmetry, and the LUMO is composed of two degenerate e orbitals (Figure 3), in accordance with Gouterman's picture of the frontier orbitals of porphyrins.[32] In addition, a state derived from the Cu $d_{x^2-y^2}$ state of b_1 symmetry is also very close to the LUMO. In the conformation with all ethyl

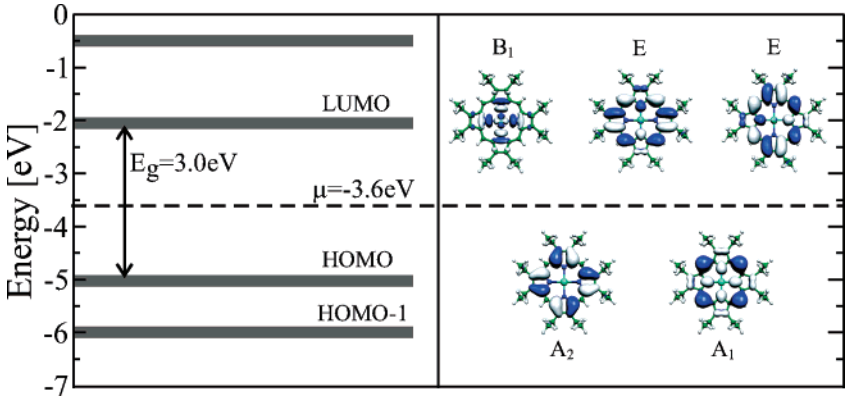

Figure 3. The computed DFT-B3LYP eigenvalues (left) and top views of CuOEP with superimposed frontier orbitals (right). The midgap position is indicated by a dashed line.

TABLE 1: Calculated Properties of the Isolated CuOEP Molecule in the Assumed Adsorbate Configuration[a]

p [D]	IP [eV]	e_{HOMO} [eV]	EA [eV]	e_{LUMO} [eV]	EN1 [eV]	EN2 [eV]
0.45	7.22	-5.11	0.6	-2.16	3.9	3.6

[a] *p*, dipole moment; e_{HOMO} and e_{LUMO}, Kohn−Sham eigenenergies of the frontier orbitals; IP, ionization potential; EA, electron affinity; EN1 and EN2, Mulliken electronegativities, calculated according to eqs 3 and 4, respectively.

"legs" pointing up, the molecule possesses a small dipole moment $p \approx 0.45$ D. The ethyl groups have a small effective positive charge, while the porphine ring is effectively negatively charged (Figure 2). We computed the vertical ionization potential (IP) and electron affinity (EA) of CuOEP by computing total energies of the singly charged cation and anion, keeping the geometry fixed, and comparing them to the total energy of the neutral molecule. The calculated ionization potential of about 7.2 eV should be compared to the experimental gas-phase value of 6.3 eV measured by Kitagawa et al.[31] The calculated value of the electron affinity is 0.6 eV, but the experimental EA is not known. Absolute Mulliken electronegativity EN can then be calculated according to its definition:[48]

$$\mathrm{EN} = \frac{\mathrm{IP} + \mathrm{EA}}{2} \tag{3}$$

Alternatively, one can use Kohn−Sham eigenenergies of the frontier orbitals:

$$\mathrm{EN} = -\frac{e_{\mathrm{HOMO}} + e_{\mathrm{LUMO}}}{2} \tag{4}$$

Even though Kohn−Sham eigenenergies have no direct physical meaning and are functional dependent, the electronegativity, obtained from eq 4, is close to the value obtained from eq 3. The two should coincide for an exact density functional.[33] Table 1 summarizes the results of our calculations. The Kohn−Sham eigenvalues for the HOMO (e_{HOMO}) and LUMO (e_{LUMO}) of the neutral molecule, ionization potential, electron affinity, and Mulliken electronegativity EN of the isolated molecule are included. Figure 3 shows the calculated Kohn−Sham eigenvalues together with 3D perspectives of the frontier orbitals. DFT-B3LYP predicts a gap of about 3.0 eV and a midgap position of 3.6 eV below the vacuum level.

4. Results and Discussion

UPS spectra of the pure substrates and of adsorbed multilayers of CuOEP in the low binding energy range are depicted in Figure 4. In all cases the binding energy is referenced to the Fermi level of the corresponding substrate. Since the sticking probability was higher on copper than on silver substrates, signatures of the metal s-band are visible in the latter case at saturation coverage. The highest occupied molecular orbital (HOMO) and the next highest occupied molecular orbital (HOMO-1) of the porphyrin are clearly resolved in all cases. We use the terms HOMO and HOMO-1 for simplicity, emphasizing their energy positions. As mentioned, HOMO (as well as HOMO-1) corresponds to two orbitals of different symmetry. Throughout this paper, we will use the positions of the maxima of the HOMO and HOMO-1 peaks as energies of these states for a more meaningful comparison with the published gas-phase data.[31] In the organic electronics literature, the upper edge of the HOMO peak is more frequently used instead, because it reflects the hole injection barrier. Figure 5 shows the evolution of the full UPS spectra upon deposition of CuOEP on the Ag(001) surface. The spectral width *W*, used to calculate work functions from eq 2, as well as the work function shift at saturation, Δ, are shown. The shift as a function of the nominal coverage, $\Delta(\theta)$, is depicted in Figure 6. The largest change (≈75%) occurs in the first monolayer, and quickly saturates at higher exposures. Measured values of the metal work functions Φ_m, ionization potentials of the molecular film IP and IP2 (corresponding to excitation from HOMO and HOMO-1), work function shifts at saturation Δ, and positions of the HOMO with respect to the Fermi level ϵ_F^v are summarized in Table 2.

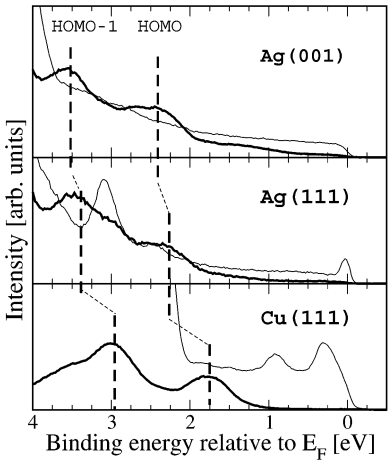

Figure 4. UPS spectra of adsorbed CuOEP multilayers in the low binding energy region (thick solid lines) compared to UPS spectra of the bare substrates (thin solid lines). Approximate positions of the HOMO and HOMO-1 states are indicated by vertical dashed lines.

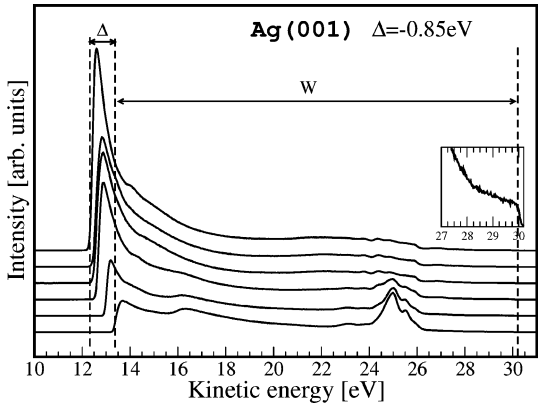

Figure 5. UPS spectra recorded with −10 V applied to the sample reveal the evolution of the low kinetic energy cutoff of the emitted secondary photoelectrons for increasing CuOEP coverage on Ag(001). The lowest spectrum corresponds to the bare substrate and the highest to the thickest multilayer. The spectra are offset in the vertical direction for clarity. The inset shows the Fermi edge of the bare substrate. The spectral width *W* and the work function change at saturation Δ are indicated.

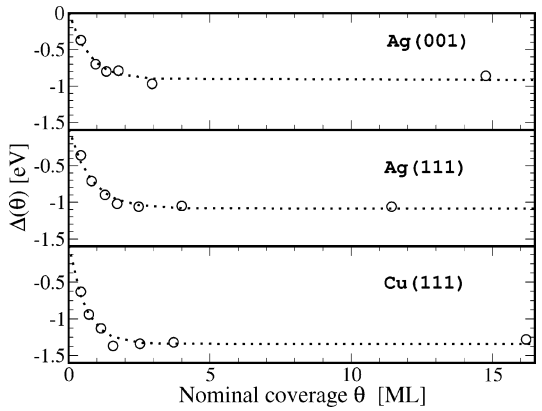

Figure 6. Work function shift $\Delta(\theta)$ as a function of the nominal CuOEP coverage θ for the three different substrates as determined from UPS measurements. Dotted lines are guides to the eye.

TABLE 2: Summary of the Main Experimental Results[a]

substrate	Φ_m [eV]	Δ [eV]	ϵ_F^v [eV]	IP [eV]	IP2 [eV]
Ag(001)	4.55	−0.85	−2.3	6.0	7.1
Ag(111)	4.62	−1.1	−2.2	5.7	6.8
Cu(111)	5.1	−1.3	−1.8	5.6	6.8
gas phase	-	-	-	6.5[31]	7.6[31]

[a] Φ_m, clean substrate work function; Δ, work function shift at saturation; ϵ_F^v, position of the HOMO with respect to the Fermi level of the metal; IP and IP2, first and second ionization potentials of the molecular film, corresponding to excitations from HOMO and HOMO-1, respectively.

We find that the measured ionization potentials of the saturated organic films are slightly different on the three substrates: 6.0 ± 0.2 eV for Ag(001), 5.7 ± 0.2 eV for Ag-(111), and 5.6 ± 0.2 eV for Cu(111). LEED patterns[25] reveal that CuOEP films on each of the two silver surfaces have a specific lateral periodicity, which is quite different from the packing in the bulk molecular crystal.[34] On Cu(111) no lateral order at highest coverage is observed. The different experimental values of IPs might therefore be due to the differences in the local environments of the molecule. All three values (6.0, 5.7, and 5.6 eV) are lower than the gas-phase ionization potential of CuOEP, 6.5 eV[31] (the average over the two lowest ionization potentials, 6.3 and 6.7 eV, which could not be resolved in our experiments). Possible origins of reduced ionization potential of molecules in the solid and in films as compared to the molecule in the gas phase have been thoroughly discussed.[35,37] The three major contributions come from (i) the screening by conduction electrons in the metal underneath, (ii) the electronic polarization of the surrounding molecules, and (iii) their vibronic relaxation, although to a much smaller extent. Screening by metal electrons is very important for the first several monolayers and decreases quickly for higher coverage.[49,50] UPS, as a surface sensitive technique, probes mainly the surface of the molecular film. Thus to extract the bulk IP, one has to correct for a small difference in screening by surrounding molecules in the bulk and at the surface. A difference, which we obtain between the gas-phase value and the value measured in the organic film, 0.5−0.9 eV, is typical for a number of organic systems.[35] A small dependence of the ionization potential of the molecular film on thin film morphology was already been observed for 4,4′-*N*,*N*′-dicarbazolylbiphenyl (CBP) on Au, Ag, and Mg by Hill et al.[36]

The variation of ϵ_F^v with respect to Φ_m is shown in Figure 7, left. It is commonly assumed[7] that the relationship is linear with a slope parameter defined as $S_B = d\epsilon_F^v/d\Phi_m$. After least-squares fit we obtain a value of $S_B \approx 0.87$. The WF shift Δ as a function of Φ_m is shown in Figure 7, right. As in the majority of other organic-on-metal systems,[7,13,12] Δ is negative. Another useful parameter, S_D, is defined as $S_D = d\Delta/d\Phi_m$. We obtain a value $S_D \approx -0.67$ after least-squares fit. The ionization potentials are slightly different for all three substrates, therefore a deviation from the usual sum rule,[12] $|S_D| + |S_B| = 1$, is observed.

In general, when $S_B = 1$ and $S_D = 0$, the WF shift Δ is constant as a function of the metal work function Φ_m. When this constant is zero, there is a vacuum level alignment at the interface (Schottky−Mott limit[12]). On the other extreme, when $S_B = 0$ and $S_D = -1$, the position of HOMO is "pinned" with respect to the Fermi level in the metal. Usually, for real systems the behavior is between these two extremes. For example, Hill et al.[12] obtained the values $S_B \approx 0.0$ for PTCDA, 0.5 for α-NPD, 0.6 for CBP, and 0.9 for Alq_3 on metal surfaces. Seki et al.[13] reported values between 0.36 and 1.0 for different tetraphenylporphyrins.

It should be mentioned that most works in the organic semiconductor community concentrated on polycrystalline metal substrates instead of single crystals, and few examples are available in the literature where WF shifts for the different faces of the same material are compared. For CuOEP we find that Δ is indeed dependent on the surface orientation: it is bigger for Ag(111), which has a larger work function (measured value 4.62 eV) as compared to Ag(001) (4.55 eV). The dependence of WF shift on the surface orientation has been long known for atomic adsorbates.[38] The physical mechanisms that lead to a VL shift upon the adsorption of closed-shell organic adsorbates are still a matter of controversy. The combination of high-precision measurements involving different techniques and calculations of the full adsorbate−substrate system is necessary for quantitative conclusions.[41] In our case such detailed information is not available, and we will therefore restrict ourselves to a semi-quantitative discussion, underlining the possible mechanisms.

It has been suggested[28,15,39,40,51] that at zero temperature the WF shift due to the first molecular layer is related to the following four contributions: (i) the decrease of the metal electron density at the surface because of the "push-back" effect, (ii) the polarization of the molecule by an attractive surface potential, (iii) intrinsic dipole moment of the organic molecule,

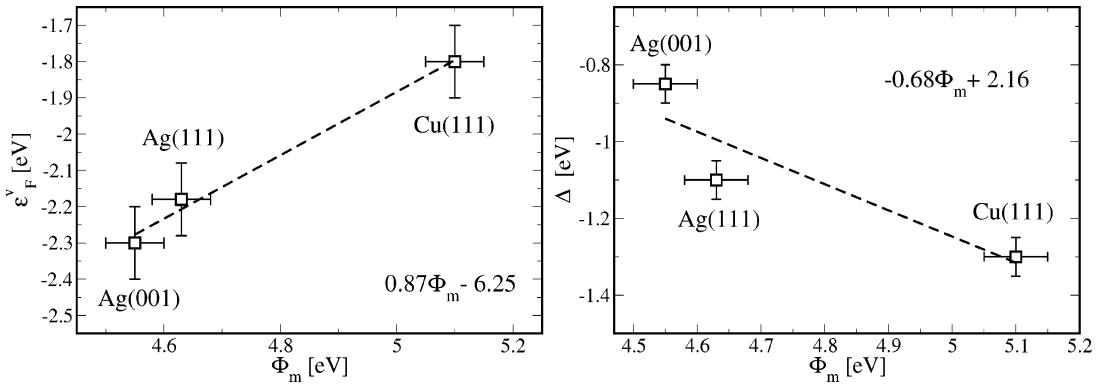

Figure 7. Left: Position of the HOMO of the organic film with respect to the Fermi level ϵ_F^v as a function of the substrate work function Φ_m. Right: Interfacial dipole at saturation Δ as a function of the substrate work function.

and (iv) charge transfer between the two interacting subsystems, i.e., the formation of the chemical bond. These contributions can sometimes be separated[14,15,39,41] and, as a first approximation, the total WF shift can then be written as the sum $\Delta = \Delta_{met} + \Delta_{pol} + \Delta_{dipole} + \Delta_{chem}$. In the absence of adsorbates, the electron density at the surface of metal spreads into the vacuum region, thus creating an interface dipole, which has a substantial contribution to the work function of the clean substrate.[38,51] Closed shell adsorbates decrease this surface dipole by pushing metal electrons back into the bulk because of Pauli repulsion. As a result, the work function is decreased, $\Delta_{met} < 0$. A closely related phenomenon is polarization of the adsorbate in the presence of an attractive surface potential,[51,52] which also leads to a lowering of work function, i.e. $\Delta_{pol} < 0$. For Xe on copper and silver surfaces, these two contributions lead to a decrease of the work function $\Delta_{met} + \Delta_{pol} \approx -0.6 \div -0.4$ eV.[38,39,53] This change is adsorbate dependent and is in general larger for more polarizable species,[43,46] e.g. aromatic molecules like ours. The contribution from the intrinsic dipole of the molecule, Δ_{dipole}, can be evaluated by using the Helmholtz relationship

$$\Delta_{dipole} = \frac{p}{\epsilon_0 A} \tag{5}$$

where p is the intrinsic dipole moment of CuOEP, and A is the surface area per molecule. The lateral periodicities and areas per molecule A of the first monolayer are known from LEED and STM measurements.[25] We find that the corresponding shifts Δ_{dipole} are -0.09, -0.08, and -0.10 eV for Ag(001), Ag(111), and Cu(111), respectively. We used the calculated value of the intrinsic dipole of the CuOEP $p = 0.45$ D. These shifts are also negative, though small, compared to, for example, the ones for methylthiols on gold, where Δ_{dipole} was shown to be the largest contribution.[41] In addition to the three mechanisms, a charge transfer between the metal and the molecular layer could occur. The chemical potential of the molecular film is approximately equal to the negative of the absolute Mulliken electronegativity:[39,40,48]

$$\mu_{mol} \approx -\mathrm{EN} \tag{6}$$

We obtain $\mu_{mol} \approx -3.6$ eV (Figure 3). The chemical potential of the metallic surface is:

$$\mu_{met} = -\Phi_m \tag{7}$$

Thus we have $\mu_{met} < \mu_{mol}$ for all three substrates and therefore charge transfer from the molecular film to the metallic substrate could be expected. For this to happen, however, metal-induced density of states at the midgap position (or, more exactly, at the so-called charge neutrality level[44]) should be large enough. In other words, coupling of molecular orbitals to the metal electronic states should be significant. This is unlikely in our case, since UPS spectra (Figure 4) show that occupied molecular states are quite far from Fermi energy and have widths smaller than 1 eV. We therefore conclude that charge-transfer contribution to the work function is less important than the sum of the previously discussed contributions.

To our knowledge, the contribution from the second molecular layer to the total VL shift (about 25% in our case) was not systematically investigated in the literature. The additional dipoles, that build up between the metal and the first monolayer, polarize the subsequent layers and therefore one expects VL change caused by the second overlayer to be of the same sign as that caused by the first overlayer. Indeed, this is the case in the majority of systems,[7] as well as in ours. Subsequent layers cause a change in WF by just a few percent.

Another interesting aspect of our results is that the total work function change for CuOEP is slightly larger than that in the case of interfaces between metals and tetraphenylporphyrins[13] (the biggest change for H_2TPP on Au reaches -1.1 eV compared to -1.3 eV for CuOEP on Cu(111)). This happens, most probably, because of the closer distance between the porphyrin ring and the metallic surface in the case of octaethylporphyrin. In fact, we know from STM measurements and DFT modeling[25] that all ethyl "legs" point upward in the first monolayer. In contrast, the phenyl "legs" do not allow for such a close contact in the case of tetraphenylporphyrins. A small intrinsic dipole of the octaethylporphyrin also contributes to Δ. An additional possible reason why the observed Δ is bigger than for other porphyrins is that single-crystal surfaces, instead of polycrystalline substrates, were used in our study. Even though in some cases VL shifts are the same for single-crystal surfaces and polycrystalline substrates,[47] a comparison of the behavior of CuOEP on two faces of the same crystal (Ag(001) and Ag(111)) shows that in general a different behavior has to be expected.

5. Conclusions

To summarize, we have studied the interfacial electronic properties of copper−octaehylporphyrin adsorbed on Ag(001), Ag(111), and Cu(111) single crystal surfaces by means of UPS. On all these substrates we have found a lowering of the work function upon molecular adsorption. The surface-dependent work function shifts are slightly larger than those for tetraphenylporphyrins on metallic substrates. This is an interesting demonstration of the effect of side groups on the energy level

alignment at the organic−metal interface. The discussion of the origin of the observed work function change shows the inherent difficulties in extracting the different contributions to that important quantity. Finding a practical recipe to determine the magnitude of all physically relevant terms will greatly help for the general understanding of organic−metal interfaces.

Acknowledgment. We thank A. Heuri for his engineering and technical support. This work was supported by the National Center of Competence in Research (NCCR) "Nanoscale Science" and the Swiss National Science Foundation.

Note Added in Proof. In ref 23, electrostatic attraction between the first molecular layer and each metal was attributed to charge transfer. Although we are now conviced that Δ is dominated by the push-back and polarization effects, the conclusions in ref 23 remain unaffected. Indeed, only a finite Δ (independent of its physical origin) is necessary for the required electrostatic molecule−substrate interaction.

References and Notes

(1) Forrest, S. R. *Chem. Rev*. **1997**, *97*, 1793. Forrest, S. R. *J. Phys. Condens. Matter* **2003**, *15*, S2599. Forrest, S. R. *Nature* **2004**, *428*, 911.
(2) Dimitrakopoulos, C. D.; Malenfant, P. R. L. *Adv. Mater*. **2002**, *14*, 99.
(3) Newman,C. R.; et al. *Chem*. Mater. **2004**, *16*, 4436.
(4) Joachim, C.; Gimzewski, J. K.; Aviram, A. *Nature* **2000**, *408*, 541.
(5) Adams, D. M.; et al. *J. Phys. Chem. B* **2003**, *107*, 6668.
(6) Zhu, X.-Y. *Surf. Sci*, *Rep*. **2004**, *56*, 1.
(7) Ishii, H.; Sugiyama, K.; Ito, E.; Seki, K. *Adv. Mater*. **1999**, *11*, 605.
(8) Ishii, H.; Oji, H.; Ito, E.; Hayashi, N.; Yoshimura, D.; Seki, K. *J. Lumin*. **2000**, *87*−*89*, 61.
(9) Knupfer, M.; Peisert, H. *Phys. Status Solidi A* **2004**, *201*, 1055.
(10) Cahen, D.; Kahn, A.; Umbach, E. *Mater. Today* **2005**, *July/August*, 32.
(11) Hirose, Y.; Kahn, A.; Aristov, V.; Soukiassian, P.; Bulovic, V.; Forrest, S. R. *Phys. Rev. B* **1996**, *54*, 13748.
(12) Hill, I. G.; Rajagopal, A.; Kahn, A.; Hu, Y. *Appl. Phys. Lett*. **1998**, *73*, 662. Δ in this paper is negative of ours.
(13) Seki, K.; Ito, E.; Ishii, H. *Synth. Met*. **1997**, *91*, 137.
(14) Peisert, H.; Knupfer, M.; Fink, J. *Appl. Phys. Lett*. **2002**, *81*, 2400.
(15) Peisert, H.; Knupfer, M.; Schwieger, T.; Fuentes, G. G.; Olligs, D.; Fink, J.; Schmidt, Th. *J. Appl. Phys*. **2003**, *93*, 9683.
(16) Campbell, I. H.; et al. *Phys. Rev. B* **1996**, *54*, 14321.
(17) Campbell, I. H.; et al. *Appl. Phys. Lett*. **1997**, *71*, 3528.
(18) Kera, S.; et al. *Phys. Rev. B* **2004**, *70*, 085304.
(19) Zehner, R. W.; et al. *Langmuir* **1999**, *15*, 1121.
(20) Scudiero, L.; Barlow, D. E.; Hipps, K. W. *J. Phys. Chem. B* **2002**, *106*, 996.
(21) Scudiero, L.; Barlow, D. E.; Hipps, K. W. *J. Phys. Chem. B* **2003**, *107*, 2903.
(22) Yoshimoto, S.; Higa, N.; Itaya, K. *J. Am. Chem. Soc*. **2004**, *126*, 8540.
(23) Ramoino, L.; von Arx, M.; Schintke, S.; Baratoff, A.; Güntherodt, H.-J.; Jung, T. A. *Chem. Phys. Lett*. **2005**, *417*, 22.
(24) Narioka, S.; et al. *Appl. Phys. Lett*. **1995**, *67*, 1899.
(25) Ramoino, L.; et al. In preparation.
(26) Berner, S.; de Wild, M.; Ramoino, L.; Ivan, S.; Baratoff, A.; Güntherodt, H.-J.; Suzuki, H.; Schlettwein, D.; Jung, T. A. *Phys. Rev. B* **2003**, *68*, 115410.
(27) Frisch, M. J.; Trucks, G. W.; Schlegel, H. B.; Scuseria, G. E.; Robb, M. A.; Cheeseman, J. R.; Montgomery, J. A., Jr.; Vreven, T.; Kudin, K. N.; Burant, J. C.; Millam, J. M.; Iyengar, S. S.; Tomasi, J.; Barone, V.; Mennucci, B.; Cossi, M.; Scalmani, G.; Rega, N.; Petersson, G. A.; Nakatsuji, H.; Hada, M.; Ehara, M.; Toyota, K.; Fukuda, R.; Hasegawa, J.; Ishida, M.; Nakajima, T.; Honda, Y.; Kitao, O.; Nakai, H.; Klene, M.; Li, X.; Knox, J. E.; Hratchian, H. P.; Cross, J. B.; Bakken, V.; Adamo, C.; Jaramillo, J.; Gomperts, R.; Stratmann, R. E.; Yazyev, O.; Austin, A. J.; Cammi, R.; Pomelli, C.; Ochterski, J. W.; Ayala, P. Y.; Morokuma, K.; Voth, G. A.; Salvador, P.; Dannenberg, J. J.; Zakrzewski, V. G.; Dapprich, S.; Daniels, A. D.; Strain, M. C.; Farkas, O.; Malick, D. K.; Rabuck, A. D.; Raghavachari, K.; Foresman, J. B.; Ortiz, J. V.; Cui, Q.; Baboul, A. G.; Clifford, S.; Cioslowski, J.; Stefanov, B. B.; Liu, G.; Liashenko, A.; Piskorz, P.; Komaromi, I.; Martin, R. L.; Fox, D. J.; Keith, T.; Al-Laham, M. A.; Peng, C. Y.; Nanayakkara, A.; Challacombe, M.; Gill, P. M. W.; Johnson, B.; Chen, W.; Wong, M. W.; Gonzalez, C.; Pople, J. A. *Gaussian 03*, revision C.02; Gaussian, Inc.: Wallingford, CT, 2004.
(28) Knupfer, M.; Paasch, G. *J. Vac. Sci. Technol. A* **2005**, *23*, 1072.
(29) Ghosh, A. *J. Am. Chem. Soc*. **1995**, *117*, 4691.
(30) Ghosh, A. *Acc. Chem. Res*. **1998**, *31*, 189.
(31) Kitagawa, S.; Morishima, I.; Yonezawa, T.; Sato, N. *Inorg. Chem*. **1979**, *18*, 1345.
(32) Gouterman, M. In *The Porphyrins*; Dolphin, D., Ed.; Academic: New York, 1978; Vol. III, Part A, Physical Chemistry.
(33) Perdew, J. P.; Levy, M. *Phys. Rev. Lett*. **1983**, *14*, 1884.
(34) Pak, R.; Scheidt, W. R. *Acta Crystallogr*. **1991**, *C47*, 431.
(35) Hill, I. G.; Kahn, A.; Cornil, J.; dos Santos, D. A.; Bredas, J. L. *Chem. Phys. Lett*. **2000**, *317*, 444.
(36) Hill, I. G.; Rajagopal, A.; Kahn, A. *J. Appl. Phys*. **1998**, *84*, 3236.
(37) Silinsh, E. A.; Capek, V. *Organic molecular crystals*; AIP Press: New York, 1994.
(38) Zangwill, A. *Physics at Surfaces*; Cambridge Unviersity Press: Cambridge, UK, 1998.
(39) Crispin, X.; Geskin, V.; Crispin, A.; Cornil, J.; Lazzaroni, R.; Salaneck, W. R.; Bredas, J.-L. *J. Am. Chem. Soc*. **2002**, *124*, 9161.
(40) Lindell, L.; et al. *J. Chem. Phys*. **2005**, *122*, 084712.
(41) De Renzi, V.; et al. *Phys. Rev. Lett*. **2005**, *95*, 046804.
(42) Lang, N. D.; Kohn, W. *Phys. Rev. B* **1970**, *1*, 4555.
(43) Da Silva, J. L. F.; Stampfl, C.; Scheffler, M. *Phys. Rev. Lett*. **2003**, *90*, 066104.
(44) Vazquez, H.; et al. *Europhys. Lett*. **2004**, *65*, 802. Vazquez, H.; et al. *Appl. Surf. Sci*. **2004**, *234*, 107.
(45) Hill, I. G.; Kahn, A.; Zoos, Z. G.; Pascal, R. A., Jr. *Chem. Phys. Lett*. **2000**, *327*, 181.
(46) Morikawa, Y.; Ishii, H.; Seki, K. *Phys. Rev. B* **2004**, *69*, 041403.
(47) Peisert, H.; Knupfer, M.; Schwieger, T.; Auerhammer, L. M.; Golden, M. S.; Fink, J. *J. Appl. Phys*. **2002**, *91*, 4872.
(48) Mulliken, R. S. *J. Chem. Phys*. **1934**, *2*, 782.
(49) Tsiper, E. V.; Soos, Z. G.; Gao, W.; Kahn, A. *Chem. Phys. Lett*. **2002**, *360*, 47.
(50) Gadzuk, J. W. *Phys. Rev. B* **1976**, *14*, 2267.
(51) Lang, N. D. *Phys. Rev. Lett*. **1981**, *46*, 842.
(52) Scheffler, M.; Stampfl, C. In *Handbook of Surface Science*, edited by Horn, K., Scheffler M., Eds.; Vol. 2, Electronic Structure; Elsevier: Amsterdam, The Netherlands, 1999.
(53) Chen, Y. C.; Cunningham, J. E.; Flynn, C. P. *Phys. Rev. B* **1984**, *30*, 7317.